Supplementary material

Porous WC-Co/N-C composite derived from PW_{12}@ZIF-67 as improved performance anodes for lithium-ion batteries

Lifei Lian,[a]* Hanbin Hu[b]*, Liang Zhang[a]

[a]Yantai Vocational College, Yantai 264670, Shandong Province, P. R. China.

[b]Yantai Tayho Advanced Materials Research Institute of Polymer New Materials Co., Ltd. Yantai 265500, Shandong Province, P. R. China.

*Corresponding author at: Yantai Vocational College, Yantai 264670, Shandong Province, P. R. China. E-mail address: lianlifei7657@163.com (L. Lian).

*Corresponding author at: Yantai Tayho Advanced Materials Research Institute of Polymer New Materials Co., Ltd. Yantai 265500, Shandong Province, P. R. China. E-mail address: Hanbinhu6715@163.com (H. Hu).

List of contents:

Experimental Section

Materials

Cobalt acetate tetrahydrate ($Co(CH_3COO)_2 \cdot 6H_2O$, AR), phosphotungstic acid ($H_3PW_{12}O_{40} \cdot nH_2O$, PW_{12}, AR), 2-methylimidazole ($C_4H_6N_2$, ≥99%, AR) were purchased from Alpha Aesar. All of the chemicals were used as received without further purification. All the reagents were used directly without further purification unless otherwise specified. All deionized water employed in the experiments was Wahaha ultrapure water.

Synthesis of the catalysts

The PW_{12}@ZIF-67 was prepared according to the literature method[1]. In brief, a mixture of cobalt acetate tetrahydrate (950 mg) was dissolved in methanol (20 mL) to form solution A. The $H_3PW_{12}O_{40} \cdot nH_2O$ (90 mg) was dissolved in water (3 mL), then added it to solution A and vigorously stirred at room temperature for 15 min. Then 2-methylimidazole (2 g) in methanol (20 mL) was quickly added, and the resultant mixture became turbid immediately. The solution was aged at room temperature for 24 h. After that, the powders were collected by centrifugation, washed by copious water and methanol to completely remove PW_{12}. The solids were dried at 60 ^oC for 12 h to afford the desired products (denoted as PW_{12}@ZIF-67).

Synthesis of WC-Co/N-C

The PW_{12}@ZIF-67 was calcinated at 700 ^oC for 3 h under N_2 conditions to form a black powder, which was washed with water (3 × 30 mL), ethanol solution (3 × 30 mL) and dried at 60 ^oC for 12 h. The product yield was determined to be 31.8%, calculated as follows: Yield = (Mass of final WC-Co/N-C product/Mass of PW_{12}@ZIF-67 precursor) × 100% (corresponding product mass: 0.318 g).

Synthesis of Co/N-C.

The Co/N-C was prepared according to the literature method[2].

Preparation and analysis of the LIB anode materials

The as prepared nanocomposites were used as anode materials for LIBs. All electrochemical performance tests were conducted at Yantai Tayho Battery Materials Technology Co., Ltd. Electrochemical measurements were performed by using coin-type cells. The electrodes were constructed by mixing the WC-Co/N-C, carbon black, and poly (vinylidene fluoride)

(PVDF) at a weight ratio of 8:1:1. The loading mass of the active materials (WC-Co/N-C) was 1 mg cm^{-2} on the electrode. This slurry was pasted on the Cu foil. The resulting foil was punched into small discs and dried under vacuum at 120 °C for 12 hours. The coin cells were assembled in an argon-filled glove box with the active material as an anode, metallic Li foil as a counter electrode, and 1 M $LiPF_6$ solution in ethylene carbonate (EC)/diethyl carbonate (DEC) (1:1) as the electrolyte. As control experiments, coin cells of Co/N-C were fabricated by the same method. CV measurements were carried out at a scan rate of 0.1 mV s^{-1} within the range of 0.01-3.0 V with an electrochemical workstation (CHI 600D). EIS was performed by using a ZAHNER-elektrik IM 6 electrochemical system over a frequency range from 100 KHz to 10 mHz. The charge–discharge measurements of cells were carried out within a fixed voltage window of 0.01-3.0 V by using a battery test system (MACCOR 4000) at room temperature [3-5].

Characterization methods

Fourier transform infrared (FT-IR) spectra were carried out on a Thermo 50 infrared spectrometer using KBr pellet method. X-ray photoelectron spectroscopy (XPS) measurements were performed using a Thermo Fisher Scientific K-Alpha spectrometer (USA). The XPS spectra were processed using XPS Peak 4.1 software with Gaussian-Lorentzian (G-L) mixed fitting functions (Gaussian fraction = 70%). For data consistency, the full width at half maximum (FWHM) of all deconvoluted peaks was constrained within ±0.2 eV. Shirley-type background correction was applied to eliminate the influence of inelastic scattering before peak deconvolution[6]. X-ray diffraction (XRD) patterns were obtained using a Bruker D8-Advanced X-ray instrument using a Cu-Kα radiation (λ = 1.5405 Å). Raman spectra were measured on a Renishaw Raman spectrometer at a laser excitation wavelength of 532 nm. BET measurements were performed at 77 K on a Quantachrome Autosorb-1C analyzer. The samples were degassed at 100 °C for 6 h before the measurements. Scanning electron microscopy (SEM) images analytical data were obtained using a Zeiss Supra 55 SEM equipped with an EDX detector. High-resolution transmission electron microscopy (HR-TEM) images were obtained on a JEM 3010 electron microscope equipped with an energy dispersive X-ray (EDX) detector. Inductively coupled plasma-atomic emission spectrometry (ICP-AES) results were measured by Thermo Fisher Scientific iCAP 7000. The electrical conductivity of the samples was measured using a PRCD3100 instrument.

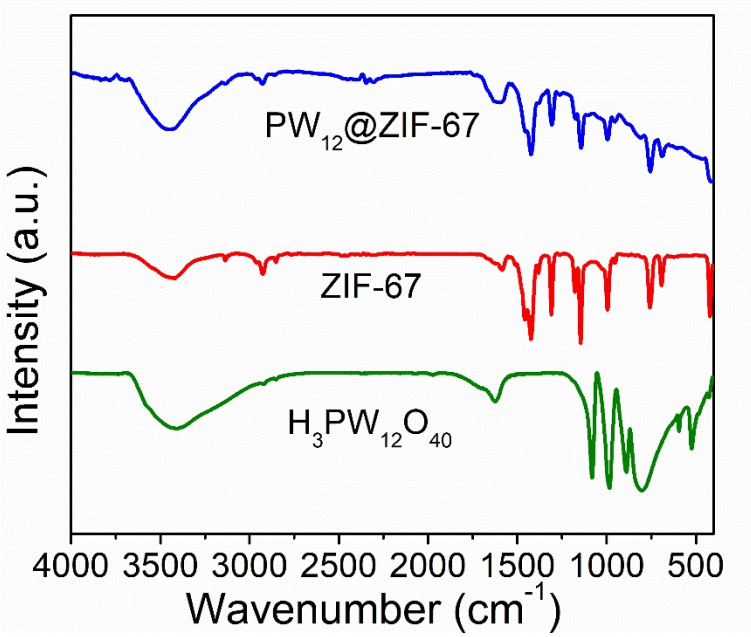

Figure S1. FTIR spectra of $H_3PW_{12}O_{40}$, ZIF-67 and PW_{12}@ZIF-67, respectively.

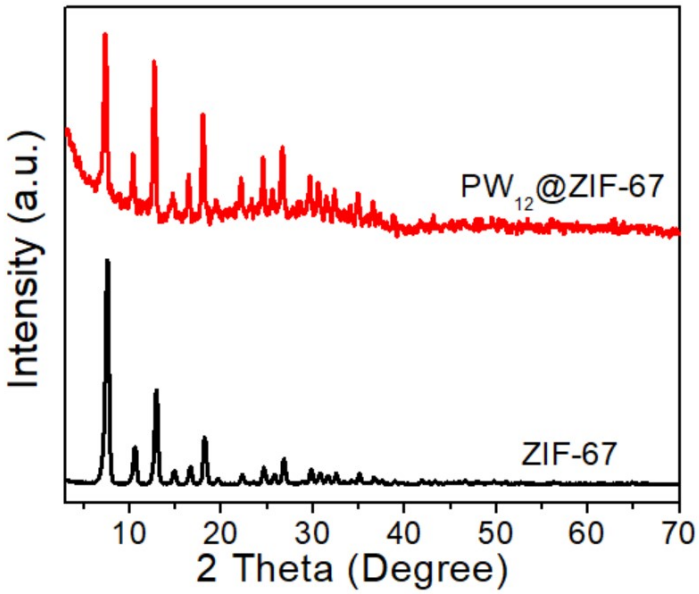

Figure S2. XRD patterns of ZIF-67 and PW_{12}@ZIF-67, respectively.

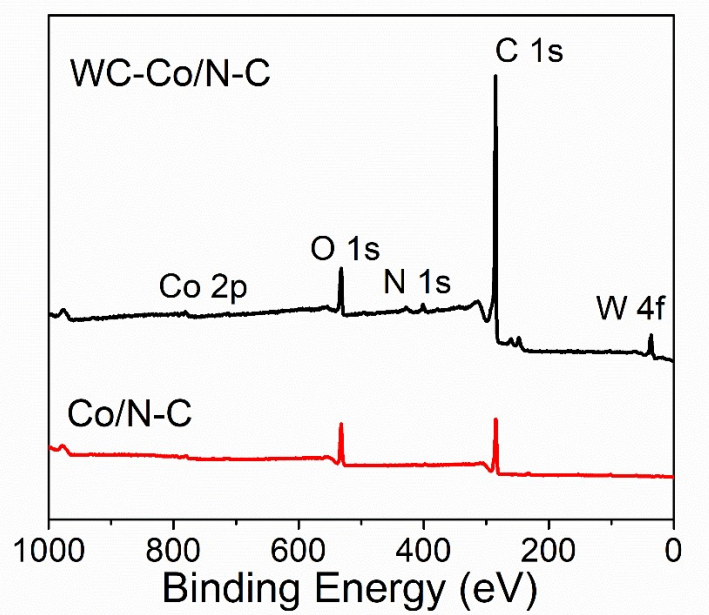

Figure S3. XPS survey spectra of WC-Co/N-C and Co/N-C, respectively.

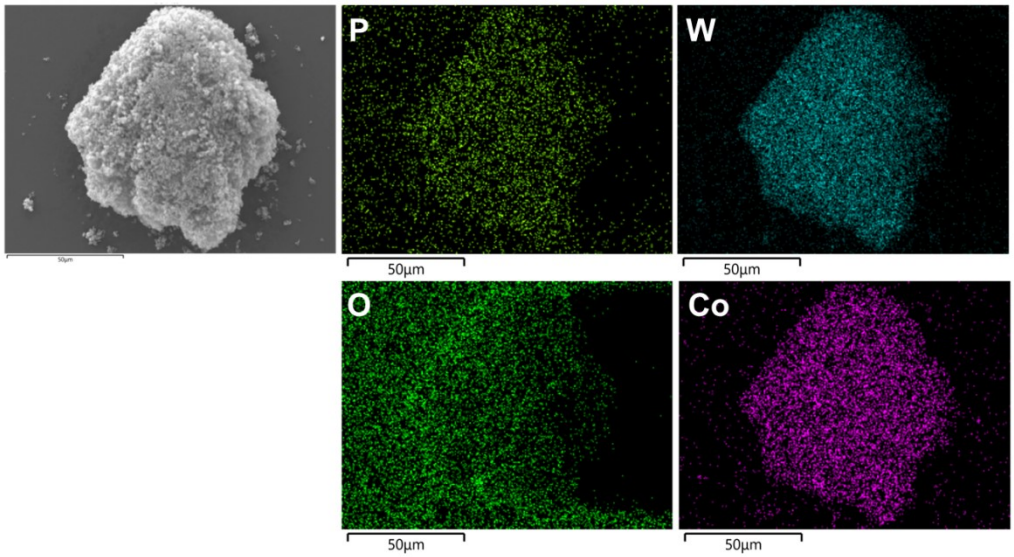

Figure S4. EDS elemental mapping data of PW_{12}@ZIF-67.

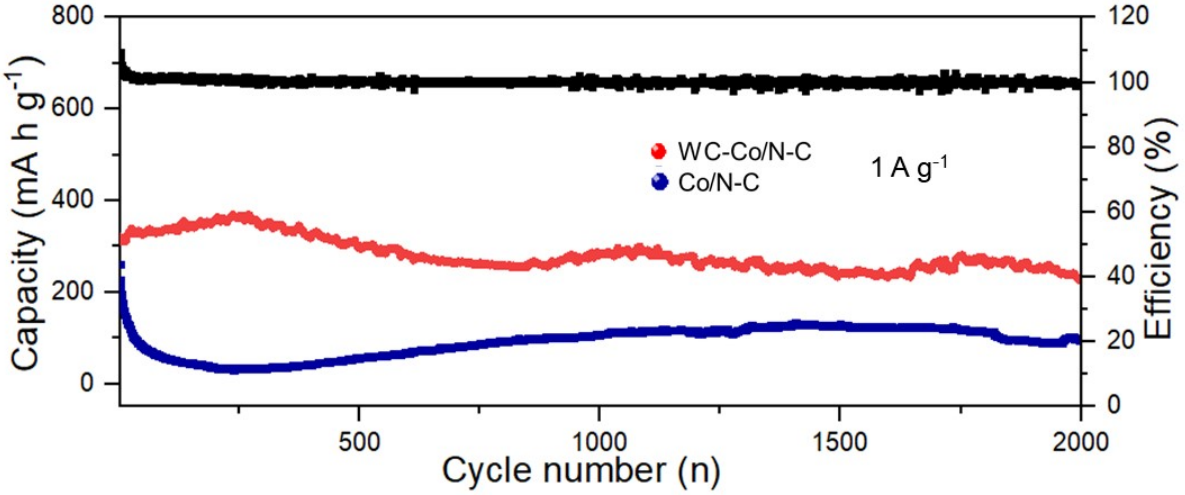

Figure S5. Cycling performance of WC-Co/N-C and Co/N-C electrode under 1.0 A g^{-1}.

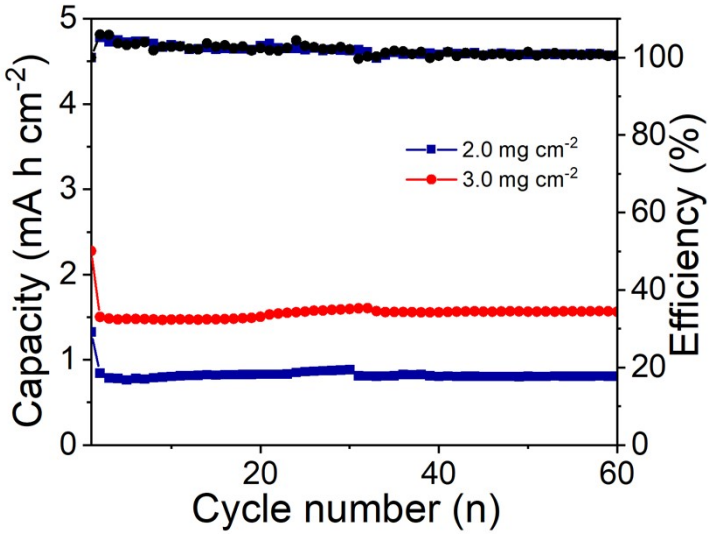

Figure S6. Cycling performance of WC-Co/N-C electrodes with different areal loadings at 0.5 A·g^{-1}.

Table S1. Specific area (S_{BET}) and Pore volume of WC-Co/N-C and Co/N-C, respectively.

Sample	S_{BET}, ($m^2 \cdot g^{-1}$)[a]	V ($cm^3 \cdot g^{-1}$)[b]	D_1 (nm)[c]	D_{BJH} (nm)[d]
WC-Co/N-C	290.18	0.53	8.9	8.4
Co/N-C	236.11	0.42	5.7	8.1

[a]BET specific surface;

[b]Total pore volume measured at P/P_0 =0.99;

[c]The average pore diameter calculated from the adsorption branch using the 4V/A (where V is total pore volume and A is S_{BET}).

[d]The average pore diameter calculated from the desorption branch of the isotherm using the BJH method;

Table S2. Inductively coupled plasma-atomic emission spectrometry (ICP-AES) and XPS quantitative analysis results for W and Co contents in WC-Co/N-C.

Analysis method	Electrode materials	C (wt%)	N (wt%)	O (wt%)	W (wt%)	Co (wt%)
XPS quantitative analysis	WC-Co/N-C	71.57	8.10	4.81	9.80	5.72
ICP-AES	WC-Co/N-C	--	--	--	12.30	7.69

Table S3. The electronic conductivity of WC-Co/N-C and Co/N-C.

Electrode materials	P (MPa)	Electronic conductivity ($S \cdot cm^{-1}$)
WC-Co/N-C	4.98	0.55
	9.98	0.76
	14.98	0.97
	19.98	1.15
Co/N-C	4.98	0.47
	9.98	0.68
	14.98	0.84
	19.98	1.03

Table S4. Comparison of WC-Co/N-C with other reported electrodes as LIBs anode materials.

Electrode materials	Current density ($mA\ g^{-1}$)	Capacity ($mA\ h\ g^{-1}$)	Cycles	Ref.
MoO_2/ZnSe@N-C	2000	252.4	--	7
Fe_2O_3/C@NCNT	1000	944.7	600	8
$Na_{0.5}Bi_{0.5}TiO_3$	100	220.0	50	9
MNC-20	100	255.0	200	10
Mo-C_{1-x}/CNF	1000	640.0	300	11
Poly(5-vinylbenzothiadiazole)	1000	164.5	500	12
$Li_{1.8}Zr_{0.8}Nb_{0.2}Cl_6$	2000	127.0	100	13
MoC_{1-x}@C	1000	657.0	500	14
WC-Co/N-C	2000	283.0	1500	This work

References

[1] L. Wang, Q. Zhang, T. Wei, F. Li, Z. Sun, L. Xu, WC and cobalt nanoparticles embedded in nitrogen-doped carbon 3D nanocage derived from $H_3PW_{12}O_{40}$@ZIF-67 for photocatalytic nitrogen fixation. *J. Mater. Chem. A.,* 2021, **9**, 2912.

[2] H. Chen, K. Shen, Q. Mao, J. Chen, Y. Li, Nanoreactor of MOF-derived yolk−shell Co@C−N: precisely controllable structure and enhanced catalytic activity. *ACS Catal.,* 2018, **8**, 1417.

[3] H. Hu, Y. Yang, X. Jiang, J. Wang, D. Cao, L. He, W. Chen, Y.-F. Song. Double-shelled hollow SiO_2@N-C nanofiber boosts the lithium storage performance of $[PMo_{12}O_{40}]^{3-}$. *Chem. Eng. J.,* 2021, **27**, 13367.

[4] H. Hu, L. Lian, X. Ji, W.-L. Zhao, H. Li, W. Chen, Haralampos N. M. Y.-F. Song, Polyoxometalate (POM)-based battery materials: Correlation between dimensionality of support material and energy storage performance, *Coord. Chem. Rev.,* 2024, **503**, 215640.

[5] J. Zhao, S. Yao, C. Hu, Z. Li, J. Wang, X. Feng, Porous ZnO/Co_3O_4/CoO/Co composite derived from Zn-Co-ZIF as improved performance anodes for lithium-ion batteries. *Mater. Lett.,* 2019, **250**, 75.

[6] M. P. Seah, M. T. Brown, Validation and accuracy of peak synthesis software for XPS, *Appl. Surf. Sci.,* 2025, **144**, 183.

[7] M. Zhong, L. Li, K. Zhao, H. Peng, S. Xu, B. Su, D. Wang, Metal-organic framework-engaged synthesis of core-shell MoO_2/ZnSe@N-C nanorods as anodes in high-performance lithium-ion batteries. *New J. Chem.,* 2021, **45**, 12064.

[8] M. Chen, F.-M. Liu, S.-S. Chen, R. Wan, X. Qian, Z.-Y. Yuan, Cactus-like iron oxide/carbon porous microspheres lodged in nitrogen-doped carbon nanotubes as anodic electrode materials of lithium ion batteries. *New J. Chem.,* 2023, **47**, 765.

[9] S. Chintha, S. Atif, A. Chaupatnaik, A. Golubnichiy, A. M. Abakumov, P. Barpanda, $Na_{0.5}Bi_{0.5}TiO_3$ perovskite anode for lithium-ion batteries, *Sustainable Energy Fuels,* 2024, **8**, 5058.

[10] J. Li, T. Ouyang, L. Liu, S. Jiang ,Y. Huang, M.-S. Balogun, Ahigh Li-ion diffusion kinetics in multidimensional and compact-structured electrodes via vacuum filtration casting. *J. Energy Chem.,* 2024, **93**, 368.

[11] J. Chen, Y. Huang, F. Zhao, H. Ye, Y. Wang, J. Zhou, Y. Liu, Y. Li, A Hierarchical a-MoC_{1-x} hybrid nanostructure for lithium-ion storage, *J. Mater Chem.,* 2017, **5**, 8125.

[12] L. Chen, C. R. Bridges, G. Gao, T. Baumgartner, X. He, Poly(5-vinylbenzothiadiazole) for high-performance lithium-ion batteries, *ACS Appl. Energy Mater.,* 2019, **2**, 10, 7315.

[13] S. Chen, M. Liu, Z. Yang, Y. Zhang, J. Liu, W. Wu, T. Huang, H. Liu, Boosting lithium-ion transport in halide solid-state electrolytes by aliovalent substitution for all-solid-state lithium-ion batteries. *Chem. Commun.,* 2025, **61**, 13429.

[14] J. Lin, J. Xu, W. Zhao, W. Dong, R. Li, Z. Zhang, F. Huang, In situ synthesis of MoC_{1-x}

nanodot@carbon hybrids for capacitive lithium-ion storage, *ACS Appl. Mater, Interfaces,* 2019, **11**, 19977.